ACS OMEGA

http://pubs.acs.org/journal/acsodf

Article

Potential Effect of Lemon Peel Oil with Novel Eco-Friendly and Biodegradable Emulsion in Un-Modified Diesel Engine

Arularasu Sivalingam,* Elumalai Perumal Venkatesan, Kenneth L. Roberts, and Mohammad Asif

Cite This: *ACS Omega* 2023, 8, 18566−18581

Read Online

ACCESS | Metrics & More | Article Recommendations

ABSTRACT: The current research work is based on exploring a novel biological fuel source and renewable fuel offered by waste lemon fruit skin. Furthermore, bio-based multi-wall carbon nanotubes (BMWCNTs), emulsion, fossil diesel, and raw lemon peel oil were procured. The single-cylinder diesel engine was evaluated using these potential ingredients in terms of performance, combustion, and emission. Test engine results reveal that the presence of BMWCNT emulsion in the bio-fuel + blend + emulsion blend produced a lower (4.7%) brake thermal efficiency (BTE) and a higher (13.6%) brake-specific energy consumption (BSEC) at peak engine load conditions with diesel. The same test fuel blend possesses an equivalent heat release rate (HRR) and cylinder pressure trends to the diesel fuel blend due to an optimized air/fuel mixture and oxygen supply. Bio-fuel + blend + emulsion achieved step-down reductions of 7.83% carbon monoxide (CO) and 20.68% hydrocarbon (HC) emissions, as well as reductions of 27.7% nitrogen oxide (NO_x) and 37.3% smoke emissions at peak engine load with diesel.

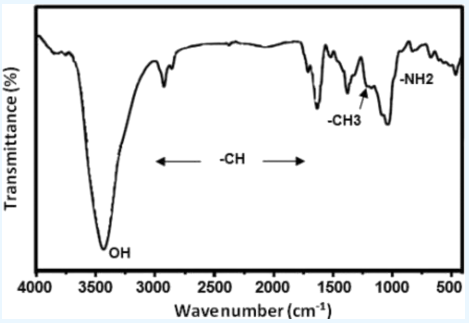

1. INTRODUCTION

It has been hard for current systems to predict how quickly global warming has been rising, and their changes have had more of an impact on nature, which has led to an imbalance in the climate.[1] Owing to this issue, numerous sectors, such as agriculture, automobiles, industrial, ocean, and seafood, as well as domestic and wild animals, were negatively affected. In particular, the increase in global warming levels leads to improved vanished glaciers, polar ice, weather events, critical issues in human healthcare, and life-threating diseases.[2] An international energy agency indicated that the vehicle sector's tailpipe emissions like carbon dioxide, carbon monoxide, and smoke were incredibly improved by 2020 and forecasted that more than 8.5 billion metric tons of CO_2 would be released in the future into the environment. Recently, half of the percentage of CO_2 was produced from the utilization of global fossil fuels, and it was not consumed by the oceans, trees, or plants but was consumed by the atmospheric air.[3]

Furthermore, this integration is involved in the carbon cycle enhancement. These anthropogenic emissions were derived from coal, oil, natural gases, carbon fuels, and agricultural matters. Emissions from fossil fuels offer added advantages for more toxic elements, and they react with air. Carbon elements remained on Earth for more than four decades, resulting in harsher ecological conditions.[4] The world's energy crisis was kick-started in the past few years due to the drop in fossil fuel sources and an uncontrolled human population, which offers massive demand in service, product, and economic sectors. This demand would be doubled by 2050. Every calendar year, about 26 and 33% of transportation- and electricity-emitted greenhouse gases, respectively, are received by the ecological system every calendar year.[5] Internal combustion engines are treated as an essential tool in the day-to-day life of modern society. It powers much of our land and sea transport, providing electrical power for farming, construction, and industrial activities. Biofuels have been gaining popularity recently as an alternative fuel for existing unmodified diesel engines.[6] Biofuels can be used in any diesel engine, usually without any modification.

It causes a reduction in toxic emissions (except nitrogen oxide (NO_x) emissions) compared to diesel fuel. Fuels of bio-origin can provide a feasible solution to this worldwide petroleum fuel crisis.[7] Biomass-derived vegetable oils are considered suitable alternates for conventional fuels.[8] However, their direct use in a diesel engine results in significantly higher smoke emissions with reduced thermal efficiency.[9] Researchers have focused on renewable energy sources since oil reserves have been consumed, and exhaust gases from motor vehicles damage the environment, atmosphere, and human health. One of the most significant sources of greenhouse gases is motor vehicles, so an investigation into the new form of energy has become essential for internal

Received: January 18, 2023
Accepted: April 28, 2023
Published: May 18, 2023

combustion engines. An experiment on diesel engines' performance and emission characteristics powered by biodiesel emulsions with additives at different load conditions has revealed substantial reduction in emissions.[10] They tested it by fueling 20% neem biodiesel with 5% water emulsion and 0.5% di-tertiary butyl peroxide, which was used as a cetane improver. It was observed a significant reduction in exhaust emissions such as NO*x*, HC, carbon monoxide (CO), and smoke. Furthermore, they noticed a 17% reduction in brake-specific energy consumption compared to the 20% neem biodiesel blend at full engine load condition. Reference 11 reviewed the water-emulsified biodiesel fuel for diesel engine applications and reported that NO_x emissions were reduced in the range of 37−50% by water-emulsified biodiesel blends operated in diesel engines. However, they also noticed that HC, CO, and specific fuel consumption was slightly improved. The titanium dioxide water-emulsified biodiesel blend for use in diesel engines was investigated.[12] They observed a higher reduction of NO_x and smoke emissions for the emulsified biodiesel blend compared to the biodiesel blend. However, they also observed a marginal increment in HC and CO emissions. The study comprehensively reviewed the effect of emulsion on diesel engine characteristics. They reported that most studies on water−diesel emulsion fuel-operated diesel engines generated lower NO_x emissions and particulate matter at all engine load conditions. Also, they noticed a slight improvement in engine performance with the emulsified biodiesel blend used in diesel engines.[13]

Researchers have focused on renewable energy sources since oil reserves have been consumed, and exhaust gases from motor vehicles damage the environment, atmosphere, and human health. One of the most significant sources of greenhouse gases is motor vehicles, so an investigation into the new form of energy has become essential for internal combustion engines. Reference 10 examined diesel engines' performance and emission characteristics powered by biodiesel emulsions with additives at different load conditions. They tested it by fueling 20% neem biodiesel with 5% water emulsion and 0.5% di-tertiary butyl peroxide, which was used as a cetane improver. They found a significant reduction in exhaust emissions such as NO_x, HC, CO, and smoke. Furthermore, they noticed a 17% reduction in BSEC compared to the 20% neem biodiesel blend at full engine load condition. Reference 11 reviewed the water-emulsified biodiesel fuel for diesel engine applications and reported that NO_x emissions were reduced in the range of 37−50% by water-emulsified biodiesel blends operated in diesel engines. However, they also noticed that HC, CO, and specific fuel consumptions were slightly improved. Reference 14 developed the optimized model for the diesel−ethanol−biodiesel fuel blends. They analyzed the various fuel blends to enhance the system profitability given production costs and fuel prices to meet the multiple fuel property criteria like heating value, kinematic viscosity, cetane number, and fuel stability. Reference 15 studied the feasibility of using lemon peel oil as a potential substitute for diesel fuel. They prepared the lemon peel oil from lemon peel rinds through the steam distillation process. They found that the lemon peel oil's viscosity is very low compared to diesel fuel. Various lemon peel blends, such as 20, 30, 40, 50, and 100%, were prepared. They found that a higher concentration of lemon peel oil added to blends showed improved engine performance and lower harmful exhaust emissions at all load conditions. Furthermore, the lower cetane index characteristics of lemon peel oil greatly influence the ignition delay period and the heat release rate. Reference 16 explored orange peel oil as a potential alternative fuel source for diesel engine applications. They determined all the physical and chemical properties of orange peel oil and compared them with diesel fuel. They found that the viscosity of the orange peel was low in comparison to other biodiesel feedstocks. The test results revealed that thermal brake efficiency was improved, and CO and HC emissions were significantly reduced at full engine load conditions with orange peel oil compared to diesel fuel.

Reference 17 examined the usage of pine oil, which was extracted from the resins of a pine tree, and it has significant fuel properties such as a lower viscosity, flash point, and boiling point than diesel. However, the fuel's cetane number is meager; therefore, the authors suggested that appending additives to pine oil was essential for diesel engine applications. Furthermore, they found a 50% blend of pine oil and diesel that showed a more significant reduction in exhaust emissions. Reference 18 investigated the viability of novel biofuel feedstocks such as *Cymbopogon flexuosus* for diesel engine applications. It was extracted through the steam distillation process. They tested various blend compositions of *Cymbopogon flexuosus* biodiesel. They also found that a 20% blend of *Cymbopogon flexuosus*−diesel has made the cars run better and cut down on pollution when they are in full working order.

However, the cylinder pressure and heat release rate were lower than diesel fuel at all load conditions. Reference 19 reviewed the less dense and lower cetane number of fuels for diesel engine use and their modes of operation. They noticed that some biodiesels, such as eucalyptus oil, pine oil, orange peel oil, and lemon peel oil, were very viscous and had fewer cetane numbers. In addition, oils made from alcohols like methanol, ethanol, butanol, ether, and pentanol were less viscous than diesel fuel. They suggested using less dense and less cetane-numbered biodiesel for future diesel engine applications due to their better physicochemical properties. Reference 20 explored the application of low viscous biodiesel such as eucalyptus oil and paradise oil in diesel engine operation. They found a significant reduction in exhaust emissions such as smoke by about 49%, 34.5% of HC, and 37% of CO for the biodiesel blend of 50% eucalyptus oil and 50% paradise oil. Oils used for biodiesel production were more preferred in terms of being edible by the community. Therefore, replacing the oilseed crops that are less well known and less used as food in society is necessary. To achieve this goal, researchers[21] must explore oil seeds produced from wild plants.

Biodiesel fuels should meet the ASTM D6751 or EN 14214 standards. Fuel properties such as cetane number, calorific value, or viscosity play an essential role in engine performance and emission testing. The CI engine was initially made to run on vegetable oil, making it perfectly suitable for diesel. Vegetable oil is not directly tested because the viscosity value is higher than diesel. Therefore, many methods are used to decrease the kinematic viscosity, such as trans-esterification, mixing with diesel, and micro emulsion.[22,23] Carried out experiments on a single cylinder, four-stroke diesel engine capable of producing a power output of 5.2 kW under varying load conditions for the blends of cottonseed oil and isobutanol with diesel fuel prepared on a volume basis, i.e., B10, B10 + 5%, B10 + 10%, B20, B20 + 5%, and B20 + 10. Results indicate that the addition of cottonseed oil increases the brake thermal

https://doi.org/10.1021/acsomega.3c00325
ACS Omega 2023, 8, 18566−18581

efficiency (BTE), reducing the 10% increase in SFC and exhaust gas temperature (EGT). CO, CO_2, and NO_x emissions were cut down, but HC emissions rose, which is bad for the environment.[24]

Reference 26 investigated the potential use of eucalyptus biodiesel as an alternative fuel in compressed ignition engines and showed that the BSFC for two different samples of B10 blend of eucalyptus diesel is about 2.34 and 2.93% lower than that of diesel fuel. The BTE for the B10 blend was found to be 0.51 and 0.94% lower than that for diesel. Some are found to be 62.5% cleaner than diesel fuel. Reference 25 experimented with the effects of pine oil and *Ceiba pentandra* methyl ester on directly injected naturally aspirated diesel engine characteristics compared with diesel fuel. The BTE increased by about 4.79% in peak cylinder pressure, heat release rate, and ignition delay. About 9.46, 16.66, 14.84, and 8.33 lowered BSFC, CO, HC, and smoke emissions, respectively. However, NO_x emissions are 8.29% higher than those of diesel. Reference 26 studied the effects of biofuel in diesel engines, and this biofuel was prepared from a mixture of waste cooking oil, 1-butanol, methanol, fossil diesel, and sodium hydroxide (catalyst). 1-Butanol was blended with biodiesel from 10 to 50% to produce the fuel blends. Furthermore, these test fuel blends were investigated with a diesel engine, and the results showed that the tailpipe emissions such as EGT, CO, HC, and NO_x were reduced at higher load conditions and engine efficiency; that is, BTE and BSFC were dropped marginally due to the addition of 1-butanol to the fuel blends. Therefore, the author recommended that this type of fuel gives the best possible results when used in a diesel engine. Reference 27 looked into the performance of biofuel/diesel blends in common rail direct injection and multi-stage fuel injection diesel engines. Oil and biofuel were mixed. Fatty acid methyl ester and mineral diesel were chosen as a fuel source, and B20 and B30 fuel blends were tested in a single-cylinder diesel engine. The engine shows higher power for B30, and both the fuel blends achieved lower fuel consumption rates compared with mineral diesel. In HC, CO, smoke, and PM emissions, the B20 blend had a minimal level and the B30 blend possessed a small increment in HC emissions. The exhaust nitrogen gas level was higher for B20 and B30 blends in comparison with mineral diesel. In terms of heat release rate and pressure, this type of fuel blend lowered the HC range compared to diesel fuel. Reference 28 analyzed the justification of carbon footprints by using oxygenated and biofuel blends to assist a post-combustion capturing system coupled with the diesel engine.

The optimized test fuel blends were conducted by mixing orange oil, Karanja oil, and oxygenated fuel. It was fueled with a zeolite-coated post-combustion system (ZCPCS) equipped with the regular single-cylinder diesel engine. Moreover, the authors have focused on the reduction of CO_2 emissions from the diesel engine. They found that the fuel blend (Karanja biodiesel) emits more CO_2 emissions than the mixture of Karanja biodiesel and orange oil, which gives a 27% drop in CO_2 emissions compared to fossil diesel. The oxygenated fuel blends (ethanol, methanol, *n*-butanol, and *n*-pentanol) were blended with a B20 blend (Karanja biodiesel + orange oil), and this blend was individually treated with ZCPCS, yielding an incredible decrement in CO_2 emissions by more than 60%. Compared to Karanja biodiesel, the oxygenated blend emitted 38% less CO_2 than the Karanja biodiesel. This is because of stoichiometric CO equilibrium. Kumar et al. utilized the sunflower waste cooking biofuel (SWCB) with oxygen enhancement in a reactivity-controlled diesel engine (RCDE) setup. The influence of raw SWCB in RCDE at higher engine loads gives a significant improvement in BTE (33.5%), and with the same engine, this blend attained a 48% decrement in smoke emission. Moreover, the authors treated the RCDE with oxygen enhancement and obtained a 36.2% higher BTE and a significant drop in emissions such as CO and HC. Still, smoke emissions show a more significant drop (37%) for the entire engine load condition. In combustion analysis (heat release rate [HRR] and pressure), the fuel blend displays a remarkable rise at peak load. The biofuel blend with oxygen supply to the RCDE has better performance and less pollution than the standard diesel engine. Reference 29 reviewed several biofuels used in diesel engines and their emissions, life cycle studies, and engine efficiency. The use of biofuel in diesel engines gives enhanced efficiency by altering the engine parameters. Suppose biofuel is used for a short time. In that case, it can replace fossil fuel utilization, and the authors noticed that biofuel could be the best fuel for short-duration operations without any significant modifications. The author also said that biofuel could be mixed with mineral diesel, additives, and esterified oil, which would make the engine run more efficiently than if it was just biofuel alone. Reference 18 assessed the performance, emission, and combustion characteristics of a single-cylinder diesel engine powered by *Cymbopogon flexuosus*. The B20 + 80% diesel resulted in higher thermal efficiency, lower HC CO, and smoke emissions. Cylinder pressure and HRR curves were lowered at full load conditions as compared with diesel fuel. Furthermore, these novel materials known as "nano additives" reduced the engine emissions. The nano additives were mixed with the fuel blends, and their properties were improved, therefore offering cleaner combustion. Recently, many researchers have used these nano additives in their engine tests as nanofuels. Reference 30 analyzed the potential effects of cerium oxide nano additives and *Cymbopogon flexuosus* biofuel in a standard diesel engine. Due to nano additives, the tailpipe emissions (NO_x, CO, HC, and smoke) declined at a higher level. Then, these nano additives also act as potential oxygen buffers and give more thermal stability, so they will increase the combustion initiating factors such as cylinder pressure and HRR. Therefore, its engine efficiency also increased to a greater extent. Reference 31 assessed the performance, combustion, and emission behavior of a diesel engine powered by ceria nanoparticle-blended emulsified biofuel. After the test engine running, its results at peak load, the BTE and BSFC for raw lemongrass oil were 24.80% and 15.2 MJ/kW-h, whereas for lemongrass oil + water emulsion, the BTE and BSFC were 26.39% and 13.8 MJ/kW-h, followed by 28.46% and 12.99 MJ/kW-h for lemongrass oil + nano water emulsion fuels, respectively. At UHC, CO emissions were reduced by 35.5 and 16.03% by the effect of lemongrass oil + nano water emulsion, and 15.69 and 26% reductions were achieved by lemongrass oil + water emulsion. It also caused lemongrass oil to have a nano-emulsion, which caused pressure and HRRs in the cylinder to go down. Reference 32 explored the application of iron (F1), aluminum (A1), and boron (B1) nano additives in fossil diesel, and then it was prepared by the sonification process. This nanofuel results in extensive flame sustenance and proper agglomeration in an ignition system, followed by a deduced ignition delay period. The engine test results revealed that the A1 nano additive attained a diminished range of cylinder pressure and fuel consumption rate with fossil diesel at a higher load. Due to the better

https://doi.org/10.1021/acsomega.3c00325
ACS Omega 2023, 8, 18566−18581

Table 1. Diverse Characteristics of Diesel Engine Powered with Various-Biodiesel-Added Emulsions[a]

biodiesel blend with emulsions	results	ref
90% diesel−10% water (water-emulsified diesel)	↑ HC, BTE and ↓ BSFC, NO_x, and smoke	25
10% water−89% soybean biodiesel−1% surfactant	↑ 6.9% of CP and HRR of15.9%↓ The exhaust emissions like NO_x, HC, CO, and smoke emission by 21.2, 16.7, 16.9, and 11.8% respectively.	19
90% heavy fuel oil−10% water	↑ 1.02% BSFC and↓ Significant reduction in NO_X emissions	20
diesel−water (5−10−15 and 20%) with constant 2% surfactant	↑ The heat release rate and cylinder pressure↓ BSFC, NO_x, CO, and CO_2	21
85% diesel−15% glucose solution	↑ HC and CO ↓ NO_x and soot emissions	22
diesel with water content range of 5 to 30%	↑ BTE and CO_2 ↓ NO_x and smoke	23
82.4% diesel−5% water−12.6% nano-organic additives	↑ BTE, HRR and CP ↓ BSFC, NO_x, and smoke	24
diesel−water (5 and 10%) with surfactant (0.5 and 2%)	↑BTE and ↓ 18.24% of NO_x	25

[a]Note: ↑ increment range and ↓ decrement range.

combustion in the engine, there was a steep increment in EGT and it strengthened the BTE for all the nano additive blended fuels compared to fossil diesel at peak load. The tailpipe emissions of CO and HC were drastically reduced by the presence of nano additives. There was a rise in the temperature of the combustion chamber because of the combustion of nano additives. This caused the NO_x emissions to be even higher. Globally, many kinds of nano additives are used in diesel engines, but there are still some unsolved problems raised by the nano additives. The use of water in nano additives led to a reduction in the fuel heating value and also damaged the test engine. The metal-based nano additives damage the ecological system and create more hazardous effects.[33] Also, the higher cost was spent on the utilization of excellent stability with nano-emulsion fuels in a diesel engine. These are all the general practical difficulties that were noticed in the previous reviews. To eliminate this practical difficulty, novel and potential initiatives were followed. Thus, the biofuel blend (biofuel + diesel + water emulsion + bio-based nano additives) was prepared to achieve better efficiency.

Presently, the entire world faces more difficulties in developing and producing new renewable energy technologies to balance the depletion of fossil fuels. The evolving "Nanotechnology" concept is considered a breakthrough and promising key to these critical issues. The nanomaterials are also called intelligent materials, and their sizes range from 1 to 100 nanometers. These materials have many such applications, and for each application, this nanomaterial was synthesized and used for the reactions. The nanomaterials were also referred to as nanofuels, nano additives, nanocrystals, nanoscale materials, bio-nano catalysts, organic nanoparticles, carbon nanotubes, single-wall carbon nanotubes, and multi-wall carbon nanotubes, followed by hybrid nano additives, nano-composites, etc. The following are the primary benefits of nanotechnology-based renewable energy products:

- Improved electrical storage size.
- Higher efficiency in heating and combustion.
- Decrement in pollution from energy production.
- Economical and safer for the ecosystem.
- By using nanotechnology in biomass, we can enhance the efficiency of biofuel and biodiesel production largely.
- Nano coatings and nanocomposites prevent corrosion and offer higher fatigue-resistant materials.

This high potential nanomaterial offers a better field of study and has broader applications in numerous products (healthcare and energy) that could enhance the eminence of human life. Nanomaterials have numerous techniques and structures, including nanocrystals, quantum dots, nanotubes, nano-fibers, carbon nanotubes, and single-wall and multi-wall carbon nanotubes. In 1985, researchers discovered an ultra-new material that originated from the mass spectra of evaporated carbon samples (sp2 carbon unit). This material has more accessible geometrical principles and offers innovative structures and symmetries; thus, for this reason, this material has much better properties with numerous applications. Meanwhile, this material was termed carbon nanotubes (CNTs), also known as one form of carbon that comes in the nano-size range. In this typical material, atoms are located in hexagonal sizes, and it has a cylindrical graphitic sheet structure trundling to the seamless cylinder in the nano-size range. Furthermore, the researchers developed the CNTs and discovered single and multi-wall CNTs. The single-wall carbon nanotubes (SWCNTs) have a single layer of graphene, and they were converted into a seamless cylinder shape with a size range of 1−2 nm.

However, multi-wall carbon nanotubes (MWCNTs) hold minimum double layers of graphene with an outside diameter of 3−30 nm and they are consistently closed at both ends. In general, the interlayer distance of MWCNTs has a nearer distance flanked by graphene layers in graphite of around 3.3 Å. Usually, the MWCNTs are synthesized by chemical vapor deposition, arc discharge, catalyst chemical vapor deposition, and laser ablation or vaporization techniques. Among various techniques for nanoparticle synthesis, the chemical vapor deposition technique achieved a higher yield, up to 100%, with the diameter ranging from 0.6 to 4 nm to 10. This material exhibits some prime properties, such as mechanical, electromagnetic, thermal, kinetic, electrical, and spectroscopic. Meanwhile, the CNT additives were blended into the prepared emulsion fuel in various proportions. The test engine results showed that the CNT-added emulsion fuel achieved higher BTE than the JME-blend emulsion fuel. Also, CNT-blended fuel showed significant depletion in HRR and in-cylinder pressure characteristics. Tailpipe emissions such as NO_x and smoke emissions were significantly reduced for the CNT + emulsion fuel blend with raw JME and emulsion fuel. In the end, the authors recommended that the usage of CNT in emulsion fuel has more potential merits in terms of efficiency and reduced emissions. Reference 34 investigated the effects of a hybrid nano-catalyst (cerium oxide + amide-functionalized multi-wall CNTs) in a biodiesel-powered diesel engine. The waste cooking oil was elected as biodiesel, and this biodiesel

https://doi.org/10.1021/acsomega.3c00325
ACS Omega 2023, 8, 18566−18581

was blended with 30, 60, and 90 ppm of hybrid nano-catalyst. The tailpipe emission of hybrid nano-catalyst-blended biodiesel (B20 + 90 ppm) attained a drastic reduction of about 18.9% (NOx), 38.8% (CO), and 71.4% (HC), followed by 26.3% (soot). Also, for this blend, the fuel consumption was cut by about 4.50%, and its thermal efficiency went up a lot more. A researcher utilized MWCNTs in a diesel engine by blending them with a jojoba methyl ester. The MWCNTs were blended with biodiesel from 10 to 50 mg/L. The author suggested that 40 mg/L of MWCNT-blended biodiesel fuel had higher performance and combustion with minimal tailpipe emissions at peak engine load. The most important findings from previous research in the proposed area were looked at, and the summaries are shown in Table 1. After evaluating the literature survey, the present engine test was conducted on bio-based multi-wall carbon nanotubes (BMWCNTs). A highly effective optimized fuel blend (fossil diesel + biofuel + water emulsion + BMWCNT) was tested with the single-cylinder diesel engine. The prime objective of this typical fuel blend is to minimize tailpipe emissions and improve engine efficiency. An aqueous type of BMWCNT was utilized as an intermediate solution to stabilize this nano additive in the inner region of the biofuel The concentration of 25 ppm (BMWCNT) was blended along with water emulsion-based biofuel.[35] Then, the diesel engine was run with the test fuel blends to figure out how the combustion, performance, and tailpipe emissions worked out for each fuel.

1.1. Novelty and Scope for the Present Research Work. The BMWCNTs were used as an additive in lemon peel biofuel (LPB) + water + emulsion + fossil diesel fuel. In this, LPB has lowered the level of viscosity and cetane number properties chosen to balance fossil fuel depletion and find the best alternative energy for the automobile sector. Besides, this LPB fuel also produces fewer emissions, so it was categorized as an eco-friendly fuel for the environment. This raw lemon peel oil was generally extracted from the renewed lemon rinds of about 8 L of LPB, which was purchased from Kothari Biofuels, Purasawalkam, Chennai, Tamil Nadu, India, and this biofuel was used as a prime source for this research work. For this reason, the scope for this biofuel was very much higher, and presently, human beings considered these lemon peels as waste and dumped them into landfills; thus, for this reason, it was available at a minimal cost. The source and availability of this raw lemon peel oil were higher in countries like India and other Asian continents.

The physicochemical properties of raw lemon peel oil and LPF were determined with the reference to ASTM and EURO norms. Based on this experimental work, there were no symmetrical research studies found. The main objective of the current experimentation is to use bio-based biodegradable nano additives blended with LPB, water emulsion, and fossil diesel, and the potential fuel blend is prepared and tested with the diesel engine in terms of combustion, performance, and tailpipe emissions. In this regard, the application of these bio-based nano additives is to reduce the engine's tailpipe emissions and improve performance. All the test results were compared with fossil diesel.

2. MATERIALS AND METHODS

The BMWCNTs were blended with biofuel and emulsion fuels and systematized by a few steps. First, industrial-grade distilled water was mixed with fossil diesel fuel and the required amount of synthesized industrial-grade BMWCNTs was procured from the Center for Nano Science and Technology, Anna University, Chennai, Tamil Nadu, India. Afterward, the procured BMWCNTs were characterized by tunneling electron microscopy (TEM), atomic force microscopy (AFM), followed by FTIR and X-ray diffraction (XRD) analyses. Then, BMWCNTs were added with the LPB and water emulsions. In this regard, the fatty acid composition of LPB was determined by GC−MS analysis. Finally, the optimized test fuel blend was obtained and the fuel was separated into individual fuel blends. Meanwhile, this test fuel blend was tested with the Kirloskar single-cylinder direct injection diesel engine at various engine load conditions. For this test, the fossil diesel (high-performance premium fuel) was procured from the local petroleum pump in Chennai, Tamil Nadu, India. This fossil diesel was utilized as a base fuel for the preparation of BMWCNTs and water emulsions. Raw LPB was generally referred to as a fuel with a lower viscosity and cetane number. This biofuel has emerged as an economical and more conspicuous fuel among all the biofuels in recent days, owing to its lighter biofuel nature. In addition, this renewable and potential source of biofuel was extracted from a variety of plants and biomass sources via pyrolysis and steam distillation techniques. Researchers observed that this biofuel had a minimal range of carbon chain lengths along with fossil hydrocarbon fuels. Fascinatingly, the heat level of LPBs attained a slightly marginal or equivalent percentage with fossil diesel, and this agreement will not produce any loss of power when raw LPB is tested in the standard diesel engine. The test fuel properties are displayed in Table 2

Table 2. Properties of Diesel and Lemon Peel Oil

fuel properties	ASTM D 6751 Test method	diesel	lemon peel oil
density (kg/m^3) at 15 °C	D 1298	833	851
viscosity (cSt) at 40 °C	D 445	3.3	1.06
calorific value (kJ/kg)	D 4809	42,500	41,512
specific gravity	D 2217	0.833	0.851
flashpoint (°C)	D 93	66	53
cetane number	D 613	74	63

2.1. Lemon Peel Oil Production. In this proposed work, the lemon peel oil is extracted from the lemon rinds through steam distillation, as shown in Figure 1. The main chamber is known as the "steam distillation chamber", which contains distilled water in its bottom part. The steam is generated from the main chamber by the use of an external heat source. The lemon peels were placed in the steam flow path, and the steam vapors heated the lemon peel rinds. The vapors consist of lemon fumes and steam particles directly supplied to the condenser unit for the cooling process. The vapors are condensed in a condenser so that the mixture of liquid water and lemon peel oil is then collected in a collecting tank. Then, the lemon peel oil is separated from the liquid water in the tank due to density variation. The collected lemon peel oil is filtered to remove the sediments. Furthermore, the lemon peel oil is washed with distilled water to remove the foam and other volatile elements. The schematic representation of lemon peel oil extraction from the lemon peel rinds is shown in Figure 1.

2.2. Detailed Characterization of BMWCNTs. For nanoparticle characterization, the required quantity of industrial-grade BMWCNTs was procured from the Center

https://doi.org/10.1021/acsomega.3c00325
ACS Omega 2023, 8, 18566−18581

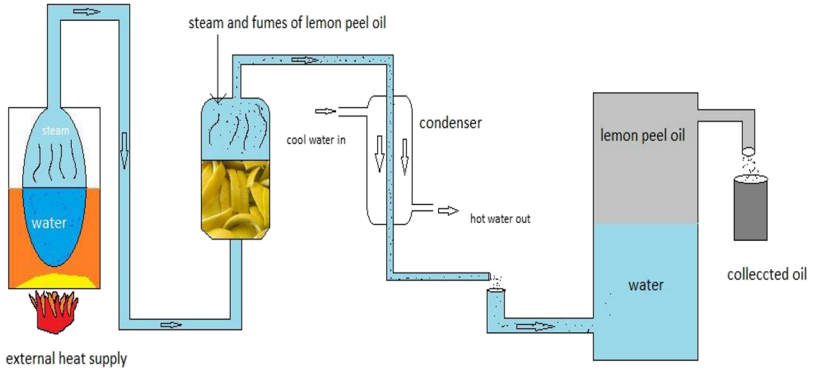

Figure 1. Lemon peel oil extraction process.

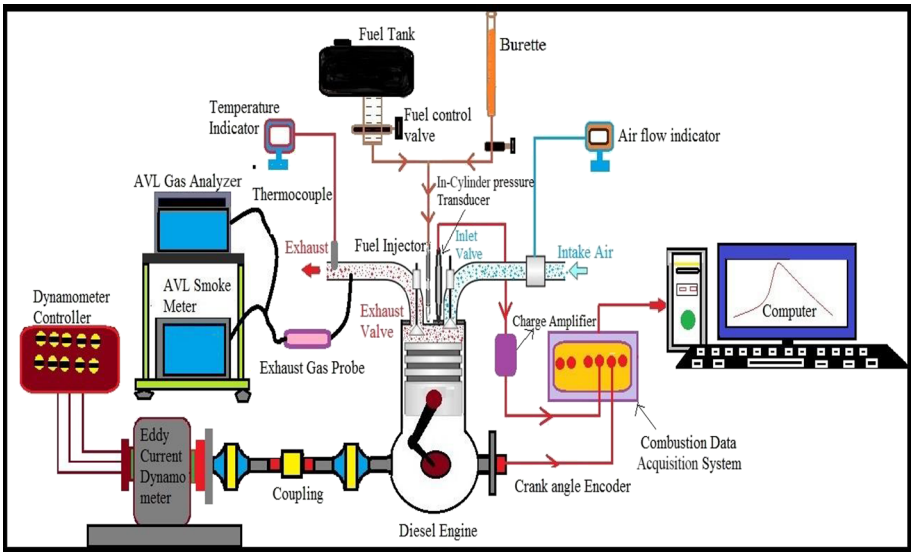

Figure 2. Schematic representation of the experimental setup.

for Nanoscience and Technology, Anna University, Chennai, Tamil Nadu, India. In the Center for Nanoscience and Technology laboratory, these BMWCNTs were prepared to assist the hydrothermal liquefaction process from the rice husk source.[36] Following that, these BMWCNTs were characterized using XRD, TEM, AFM, and FTIR (Fourier-transform infrared spectroscopy). Then, the lemon peel oil was subjected to GC−MS (gas chromatography−mass spectrometry). Afterward, the Philips PW instrument was used for XRD analysis to determine the diffraction pattern of BMWCNTs with 40 mA, 45 kV, and Cu Kα (1.458) radiation. Then, the aggregation, BMWCNT nano additive morphology, and size were obtained by TEM (CM12 Philips 2016 model under 200 kV acceleration voltage).

For in-depth characterization, the ultra-modern, high-accuracy AFM was used with the setup of the Veeco instrument linked with nanoscale 6, HarmoniX, and the controller system. The sample was placed in the wafer medium (Si/SiO_2) with the admission of a few drops onto the wafer. For this analysis, deionized water was obtained from Zeneer Power 1 UV−Scholar under 18.9 MΩ. The FTIR system and a Ni-Chrome source, Magna 750 FTIR fixed with a deuterated triglycine sulfate detector (make: Japan) were used to analyze the LPB and BMWCNTs. The optimized range of FTIR is from 500 to 4000 cm^{-1} with a 2 cm^{-1} resolution. Besides, GC−MS was used to study the FAME (fatty acid methyl esters) of raw lemon peel oil at 350 °C about a 12 min reaction time.

2.3. Uncertainty. The uncertainty in any measured parameter was estimated based on the Gaussian distribution method with confidence limits of +2σ (95.45% of measured data lie within the limits of +2σ of mean). Thus, the uncertainty was estimated using the following equation: uncertainty of any measured parameter (ΔXi) = $2\sigma i/\overline{X} \times 100$.

Experiments were conducted to obtain the mean ($\overline{X}i$) and standard deviation (σi) of any measured parameter (Xi) for a number of readings. This was done for speed, load, and time for a specified amount of air and fuel to flow.

For the analysis, 20 sets of readings have been taken at the same engine operating condition. The uncertainty value for speed, load, airflow reading, fuel flow reading, and EGT, NO emission, HC concentration, and O_2 concentration are calculated based on eq 1.

From the uncertainties of the measured parameters, the uncertainties in computed parameters are evaluated by using an expression, which is derived as follows.[37]

Let R be the computed quantity from n independent measured parameters $X1$, $X2$, $X3$, ..., Xn.

Thus, $R = R\ (X1, X2, X3,...)$

Let uncertainty limits for the measured parameters be $X1 + \Delta X1$, $X2 + \Delta X2$, $X3 + \Delta X3$, ..., $Xn + \Delta Xn$ and the uncertainty limit for the computed value be $R + \Delta R$.

https://doi.org/10.1021/acsomega.3c00325
ACS Omega 2023, 8, 18566−18581

In order to get realistic error limits for the computed quantity, the principle of the root sum square method is used and the magnitude of the error is given by

$$\Delta R = [((\partial R/\partial X1 \times \Delta X1)^2 + (\partial R/\partial X2 \times \Delta X2)^2 + \cdots + (\partial R/\partial Xn \times \Delta Xn)^2)\ldots]^{1/2} \quad (1)$$

Using eq 3 for a given operating condition, the uncertainties in computed quantities such as mass flow rates of air and fuel, equivalence ratio, brake power, and BTE are estimated.

2.4. Experimental Diesel Engine Setup. The entire experimental work was conducted on Kirloskar's single-cylinder direct injection diesel engine, which is primarily used for agricultural purposes. This engine developed 3.5 kW of power, and it was operated at a constant speed of 1500 rpm. This diesel engine had a fuel capacity of 7 L and a stroke and bore of 112.75 and 88.7 mm, respectively, along the connecting rod. As per the engine manufacturer's specifications, this engine was operated at 17:1 (compression ratio), 200 bar (injection pressure), and 23° bTDC (injection timing). For this experiment, the MICO-based fuel injection system and piezoelectric pressure transducer were used to analyze the diesel engine's combustion characteristics (HRR and in-cylinder pressure). The QRO-402 exhaust gas analyzer was used to test the tailpipe emissions such as HC, NO_x, and CO, and the smoke opacity was measured by the AVL 437C smoke meter. The entire engine setup image is displayed in Figure 2. The engine load was coupled with an eddy current dynamometer to deliver the load to the engine, and this engine was operated from a lower to higher load condition based on the varied current supply. The whole experiment was done with 0 to 100% load conditions at intervals of 25%. The test engine was cooled via natural air, while SAE 40 lubricating oil was used with a maximum of 3.8 L at 85 °C to avoid wear and tear problems between the engine components. Table 3 reveals the engine specifications for this diesel engine. Meanwhile, to constantly check the heat release of engine oil, tailpipe emissions and how much heat was delivered to the atmosphere were calculated by the temperature sensors fitted to the engine. Then, the uncertainty analysis of various instruments and parameters is presented in Table 4.

Table 3. Technical Details of a Test Setup

parameter	specification
make	Kirloskar TV1
description	four-stroke, single-cylinder, water-cooled direct injection diesel engine
speed	1500 rpm
rated power	4.4 kW
stroke volume	661 cc
cylinder diameter	87.5 mm
stroke length	110 mm
compression ratio	17.5:1
fuel injection timing	23° bTDC
fuel spray angle	120°
no. of nozzles	03
diameter of the nozzle hole	0.3 mm
geometry of piston	hemispherical
inlet valve open	4.5° bTDC
inlet valve close	35.5° aBDC
exhaust valve open	35.5° bBDC
exhaust valve close	4.5° aTDC

Table 4. List of Instruments with Their Range, Accuracy, and Uncertainties

instrument	measurement	range	accuracy	uncertainty
AVL 444N five gas analyzer	CO	0 to 10% vol	±0.03%	±0.2%
	CO_2	0 to 20% vol	±0.5%	±0.15%
	HC	0 to 20,000 ppm	±10 ppm	±0.2%
	O_2	0 to 22% vol	±0.1%	±0.5%
	NO_x	0 to 5000 ppm	±50 ppm	±1%
AVL 437C smoke meter	SO	0−99.9	±1%	±1%
AVLGH14d/AH1 pressure transducer	pressure	0−100 bar	±0.1 bar	±0.15%
AVL 365C angle encoder	crank angle	0−720°	±1%	±0.2%
data acquisition system	combustion characteristics	12 bit	±0.01 bit	±0.01%
temperature indicator	temperature	0−900 °C	±1 °C	±0.2%

3. RESULTS AND DISCUSSION OF THE EXPERIMENT

3.1. Bio Assisted Nano-Emulsion Fuel Preparation and Its Characterization. For the test fuel preparation, the biofuel (LPB) and nano additives (BMWCNTs) were blended with the transitional solution (H2O) to reduce the stability nature of the nano additives. To soothe the water in diesel fuel, the fatty acids act as lipophilic mediators, and the neutral salt was used in this reaction as a hydrophilic mediator. For the preparation of emulsion fuel, approximately 8 cm^3 of oleic acid, 12 vol % water fossil diesel, and 0.9 cm^3 of monoethanolamine solution were placed in a half-liter container and stirred at a speed of 1000 rpm. The formation of fatty acid salt occurred due to the nature of the hydrophobic solution phase. Meanwhile, for the preparation of a highly stable water-fossil diesel emulsion, about 85 cm^3 (fossil diesel), 15 cm^3 (H2O), and 2.5 cm^3 (*n*-hexanol) were mixed along with the hydrophobic solution and this mixture was taken for the stirring process at 1000 rpm for 5 to 15 min. Through this stirring process, the H2O droplets were present in the homogeneous fossil diesel fuel. The water-fossil diesel emulsion was stored in the container for further usage. Next, about 15% of water-fossil diesel emulsions were poured into the glass container, followed by adding 80% of LPB into the same container so that a 5% (water fossil diesel emulsions) + 80% of LPB + 15% (fossil diesel) fuel blend was attained. Finally, 25 ppm of BMWCNTs was blended with the previous fuel blend, and this prepared test blend was tested in the diesel engine. All the test results were compared with raw fossil diesel fuel for performance and emission characteristics.

3.2. Characterization of BMWCNTs. In general, MWCNT belongs to nanomaterials and it is used in industrial mass production due to its excellent electrical and mechanical properties. The base structure of CNTs was synthesized by converting sp2 carbon elements into simple geometrical principles, and it attains an ultra-new, enthralling base structure with incredible applications. Initially, the BMWCNTs were procured from the Center for Nanoscience and Technology, Anna University, Chennai, Tamil Nadu, India. Then, a hydrothermal process was applied to prepare the BMWCNTs. Subsequently, the procured BMWCNTs were characterized by

https://doi.org/10.1021/acsomega.3c00325
ACS Omega 2023, 8, 18566−18581

TEM, AFM, and Fourier transform infrared (FTIR) spectroscopy followed by XRD, and the raw LPB fatty acids were analyzed by gas chromatography (GC).

3.2.1. TEM. Initially, the prepared sample was positioned in column 1 to analyze the loaded sample. Figure 3 reveals the

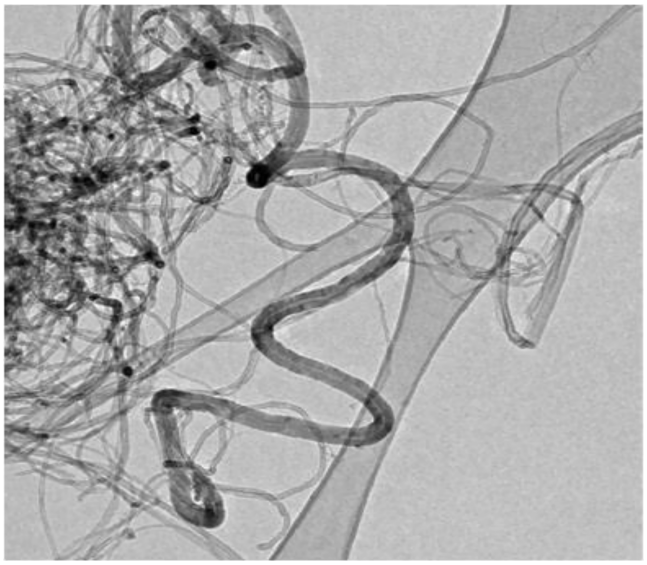

Figure 3. TEM spectroscopy image of BMWCNTs.

TEM spectroscopy image of BMWCNTs having a cylindrical tube-like structure (nanotube) with aggregation, and their threads were snarled against each other. This agreement confirms the presence of BMWCNTs in the sample within a 30 nm range. The high aspect ratio and strong van der Waals interactions result in entangled and bundled BMWCNTs. Thus, the dispersion of BMWCNTs is a challenging task for their utilization in nanoscale device applications. The poor dispersion of BMWCNTs in organic solvents and water has restricted their applications. In organic solvents and polymers, the BMWCNTs were dispersed in more prospective applications in nanoscience. The BMWCNT dispersion in isopropyl alcohol was carried out, and the high-resolution TEM image indicated that the diameter was 30 nm, with slightly dispersed tubes. The maximum aggregation of BMWCNTs was observed by TEM analysis in hexane solvent, with an outer diameter of about 40 nm.

3.2.2. AFM. The AFM image is displayed in Figure 4. Before the AFM analysis, the samples were placed on the Si/SiO2 substrate and it was taken for analysis. Then, the AFM image confirms that the sample has enlarged the image of a cylindrical rod-type shape (nanotube) in the 4.5−6 nm range. Besides, the image reveals that the presence of biomolecules on the BMWCNTs produces a broad tube-like structure and this orientation was identified by AFM spectroscopy. AFM is much more widely used in the study of soft samples such as polymers and biological systems. One of the main limitations of the AFM is that it is difficult or even impossible to relocate the same feature, object, or region of interest within a sample once the probe tip is lifted or the substrate is rotated or moved.

A high-precision relocation technique is needed for a great many applications. One of the most critical applications of the AFM is in the research of changes in samples. The Digital Instruments Multimode III SPM AFM was performed in tapping mode. The height and phase images were recorded

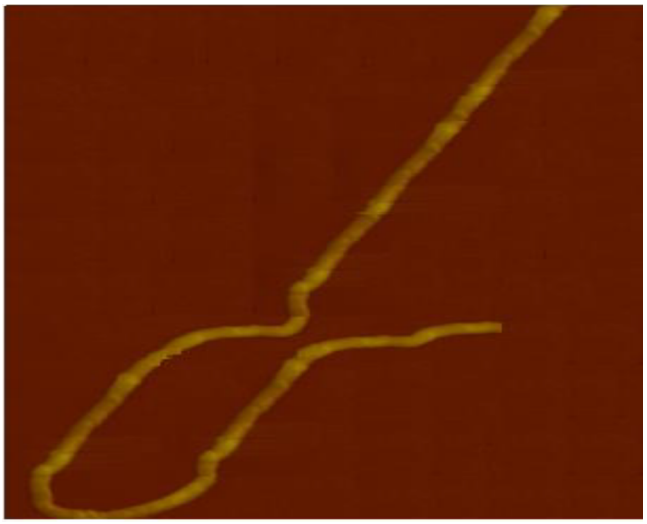

Figure 4. Atomic force microscope image of BMWCNTs.

simultaneously under moderate tapping conditions (set-point ratio rsp ≈ 0:70) with an accessible amplitude of 80 ± 10 nm, a scan speed of 1.0 Hz, and several samples of 512 × 512. The operating frequency was re-adjusted after engaging the tip on the surface. The operating frequency was kept on the low-frequency side of the resonance during the imaging. Commercial silicon probe tips with a spring constant of about 50 nm were used.

3.2.3. FTIR. FTIR spectroscopy has been extensively used in the structural determination of molecules and in identifying the functional groups attached to the surface of the BMWCNTs. Thus, using FTIR spectra, the presence of carboxyl (−COOH), carbonyl (−C=O), and hydroxyl (−OH) functional groups bonded to the ends and sidewalls of the CNTs was confirmed. The sample was loaded into the FTIR spectroscope, and hence the relevant peaks for BMWCNTs were generated, as shown in Figure 5. The BMWCNTs have

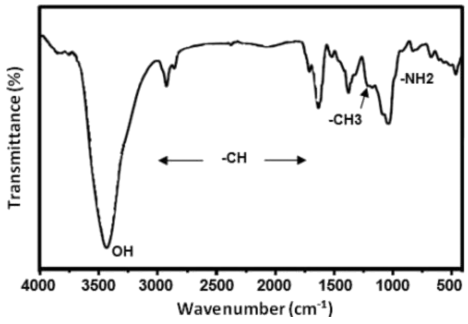

Figure 5. FTIR spectroscopy of BMWCNTs.

some feeble peaks from 1700 to 3000 cm^{-1}, which is consistent with the −CH band. FTIR spectroscopy results in the N−H band at 1236 cm^{-1}. This agreement supports the presence of biomolecules besides BMWCNTs. Then, the sharp peak of 3492 cm^{-1} reveals the existence of the N−H band in the sample, and it was broader than other generated peaks in this region, namely, aromatic ring and carbonyl stretching modes. The scissors-in-plane twisting approach of the NH_2 amine group is available at 1746 cm^{-1}. The wide-ranged band at 992 cm^{-1} appeared owing to the NH_2 mode. The generated peaks, 1258 and 2892 cm^{-1}, were related to the absorption bands

https://doi.org/10.1021/acsomega.3c00325
ACS Omega 2023, 8, 18566−18581

−CH3 and C−H. The peak of 1256 cm^{-1} fits the C=O absorption stretch. Some other minor peaks were related to C−CO−O, C−CH3, and −CH3. The FTIR results agreed that the BMWCNTs were present in the loaded sample. The wide transmission band at 3450 cm^{-1} observed in both BMWCNT-OH and BMWCNTCOOH spectra is primarily due to the vibration mode of hydroxyl groups (OH). The BMWCNTs clearly show oxygen-containing groups resulting from oxidation processes: a broadband centered around 3450 cm^{-1} can be ascribed to O−H stretching vibrations in C−OH groups, and the −OH characteristic band appeared significantly broad and with higher intensity.

This increase in intensity is attributed to the increase in some hydroxyl groups on the BMWCNTs. The appearance of new characteristic peaks at 3450 and 3550 cm^{-1} was observed in the spectra of hydroxyl and carboxyl groups of functionalized BMWCNTs, while it was negligible in the untreated BMWCNTs. This kind of band can be attributed to the stretching vibration of carbon−oxygen bonds (C=O). These observations indicate the existence of −OH and −COOH groups on the surface of MWCNTs.

3.2.4. XRD. Figure 6 displays XRD analysis of BMWCNTs, and the deflection peaks at 2θ of 40, 46, and 66 are related to

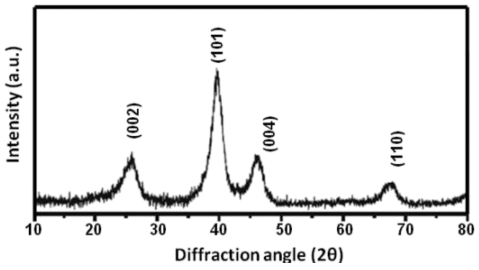

Figure 6. XRD analysis of BMWCNTs.

(1 1 1), (2 0 0), and (2 2 0) planes in association with a previous research finding.[38] The deflection peak (1 1 1) mean particle size was evaluated by Scherrer's method.[39] Then, the chronic mean particle size of BMWCNTs was in the 5.2 nm range. Finally, the result agreed on the presence of BMWCNTs in the sample at an appropriate nanometer size and it will aid in upgrading the reaction's catalytic activity. The presence of diffraction peaks at 2θ values of 25.6, 26.2, and 26.1° corresponds to the diffraction plane (0 0 2) and confirms the highly graphitic structure of the MCNT particles. The peak (0 0 2) attained in the XRD pattern of BMWCNTs is due to interlayer stacking of grapheme sheets. It indicates the concentric cylindrical nature of graphene sheets nested together, and the nanotubes are multi-walled. XRD results of pure BMWCNTs show four characteristic peaks at 25.6° (0 0 2), 40.0° (1 0 1), 59.0° (0 0 4), and 71.0° (1 1 0) (JCPDS card no. 41-1487). The peak width and peak intensity vary significantly depending upon the functionalization of the BMWCNT surface. These changes could be correlated with the variation in d spacing and lattice distortions due to the defective stacking of tubules. Carboxyl and hydroxyl treatments affect the carbon structures on the surface of the BMWCNT due to oxidation/surface interaction, thereby leading to lattice distortions. The average spacing values calculated using Bragg's law lie in the range of 3.44−3.47 Å.

4. ENGINE TEST RESULTS

4.1. Brake-Specific Energy Consumption (BSEC). BSEC indicates the energy consumption from input fuel based on the obtained shaft power from the test engine. The energy consumption rate depends on various factors such as the property of the test fuel, combustion chamber temperature, engine load, and pumping losses. From Figure 7, it is observed

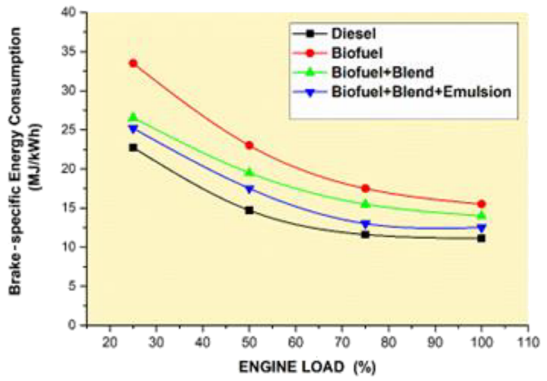

Figure 7. BSEC for various fuel blends.

that pure biofuel exhibits the highest BSEC of about 31.6, 23.2, 16.4, and 15.12 MJ/kW-hr at engine loads of 25, 50, 75, and 100%, respectively. With an increase in engine load, the BSEC tends to be reduced due to improved engine temperature, evaporation rate, and efficiency. Neat biofuel exhibits high energy consumption due to fatty acid chains in non-emulsified oil, resulting in a lower vaporization rate, poor volatility, and deteriorated combustion.[40] At the same time, the emulsified blend exhibits better energy consumption due to secondary droplet atomization and the micro-explosion phenomenon.[41] Furthermore, the appending of additives resulted in improved atomization and evaporation rates in emulsified fuel. In comparison with all the fuel blends, the nano additives blended emulsion fuel blend has dropped a range of fuel consumption. This same blend had slightly (13.6%) higher fuel consumption compared with mineral diesel. This could be because the cumulative effect of the nano additives on the micro explosion occurrence could be declared as the main reason for such enhancements. These could collectively make uniform the air−fuel mixture in the combustion chamber, lowering the ignition delay and shortening the combustion duration of fuel and thereby improving the brake power at full load. Efficient fuel atomization, fuel evaporation, and air−fuel mixing on the one hand and decreased ignition delay on the other hand compensated for the unfavorable impact of water addition, i.e., reduced energetic content of the waster-emulsified fuel blends. These improvements were more pronounced for fuel blends, which could be justified by the higher energetic content of the fuel blend caused by the addition of the nano additives.

4.2. BTE. The BTE indicates the efficiency of the test engine in retrieving energy from the combusted fuel via the indicated energy output. As shown in Figure 8, it is observed that BTE increases with an increase in engine load owing to improvements in in-cylinder chamber temperature, fuel atomization, and higher mechanical efficiency. Factors responsible for BTE are calorific value, cetane number, kinematic viscosity, and the amount of oxygen content in the test fuel. The highest BTE is observed for diesel fuel (31.92%)

https://doi.org/10.1021/acsomega.3c00325
ACS Omega 2023, 8, 18566−18581

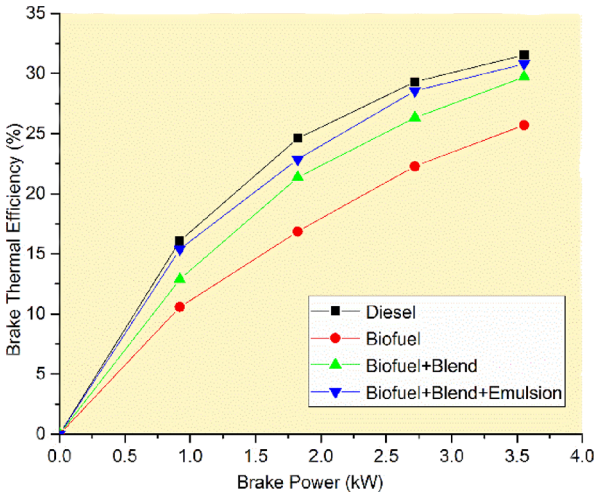

Figure 8. BTE for various fuel blends.

due to optimum air−fuel mixture, volatility, and optimum fuel viscosity, resulting in incomplete combustion. Neat biofuel is found to exhibit a lower BTE compared to other test fuels due to the presence of fatty acid chains, resulting in poor combustion. This could also be attributed to poor air−fuel mixing, higher volatile nature, diminished spray characteristics, and lowered calorific value.[38] Due to the micro explosion phenomenon and the emulsified fuel's secondary atomization, BTE is improved. However, the occurrence of secondary droplet formation can be traced to the evaporation of water molecules at higher in-cylinder temperatures. Applying additives in emulsified fuel results in improved atomization and vaporization of fuel droplets, subsequently improving the BTE.

The presence of additives initiates the mixing of air and fuel inside the engine cylinder to make the combustion complete, thus increasing the engine's thermal efficiency. The addition of nano additives in the fuel blend substantially improved the BTE of the emulsion fuels and, compared with diesel fuel, biofuel + blend + emulsion blend, possessed a 4.7% lowered BTE peak load. This was due to the catalytic activity of the nano additives, leading to higher combustion temperatures and, subsequently, more efficient evaporation of the existing water molecules. This could, in turn, intensify the micro-explosion phenomenon and secondary atomization, propelling the combustion process toward more completion and increasing BTE. These results agreed with those reported in the published literature on the utilization of nano additives in water-emulsified fuels. The test results revealed that an enhanced BTE can be obtained with the emulsion fuel. This is mainly due to the micro explosion phenomenon, i.e., the instantaneous and rapid vaporization of the water droplets within the fuel droplets. The fuel is exposed to high-temperature gas, and large fuel droplets are broken into many smaller droplets, thereby significantly improving fuel vaporization and the combustion process. For instance, ref 42 utilized the CNTs in Jatropha methyl ester (JME) emulsions and tested them with the diesel engine. Then, the JME-blended emulsion was prepared with 93% raw JME, 2% surfactants, and 5% water mixed with a hydrophilic−lipophilic balance solution.[43] Also, the authors reported that improvements in BTE, particularly at elevated engine loads, were due to CNT incorporation into water-emulsified biodiesel. They attributed the increase in BTE with the increase in fuel−air mixing degree in the presence of CNTs. In a different investigation, the presence of CNTs in water/biodiesel fuel emulsions was found to reportedly decrease the ignition delay, thereby minimizing fuel consumption. They also emphasized that CNTs intensified the micro-explosion phenomenon and consequently improved the BTE of the water-emulsified fuels.[44,45]

4.3. Cylinder Pressure. It is observed that diesel fuel shows the highest in-cylinder pressure and HRR in comparison with other test fuels due to a lower premixed combustion phase (PCP). Raw biofuel tends to exhibit lower in-cylinder pressure due to fatty acid chains in non-emulsified test blends, thereby leading to poor vaporization and volatility, followed by poor combustion. Moreover, the emulsified biofuel blend exhibits higher in-cylinder pressure compared to raw biofuel and additive-appended biofuel due to the presence of water molecules, causing an increase in ignition delay period, thus causing more accumulation of fuel in the combustion chamber followed by improper fuel burning during combustion.[46−50]

Emulsified fuel with additives showed lowered cylinder pressure, resulting in a lower premixed phase. The nanoparticle presence in the water/biofuel emulsion fuel enhances the heat transfer properties and reduces the IDP during the combustion process. In comparison with mineral diesel, all the fuel blends had a lower range of in-cylinder pressure. This could be owing to the better burning characteristics and shorter ignition delay attributes of additive blended emulsion fuels. Similarly, emulsified fuel had a minimal HRR in comparison with diesel fuel and additive-appended emulsified fuel because of the lowered cetane number of emulsified fuels along with a longer ignition delay. However, the addition of additives increases the cetane number and causes a delay in ignition. As shown in Figure 9, at 100% engine load, the cylinder pressure of diesel

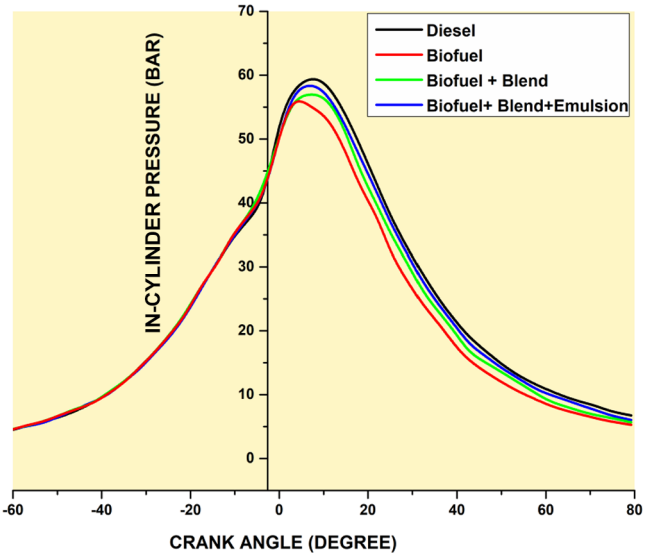

Figure 9. Cylinder pressure for various fuel blends.

fuel is 59.86 bar, whereas for the biofuel, emulsified biofuel, and additive-appended emulsified fuel, the cylinder pressures are about 56.9, 57.2, and 58.2 bar, respectively.

4.4. HRR. The correlation considered the HRR at every crank angle for different test fuel blends from the first law of thermodynamics by the following equation:

https://doi.org/10.1021/acsomega.3c00325
ACS Omega 2023, 8, 18566−18581

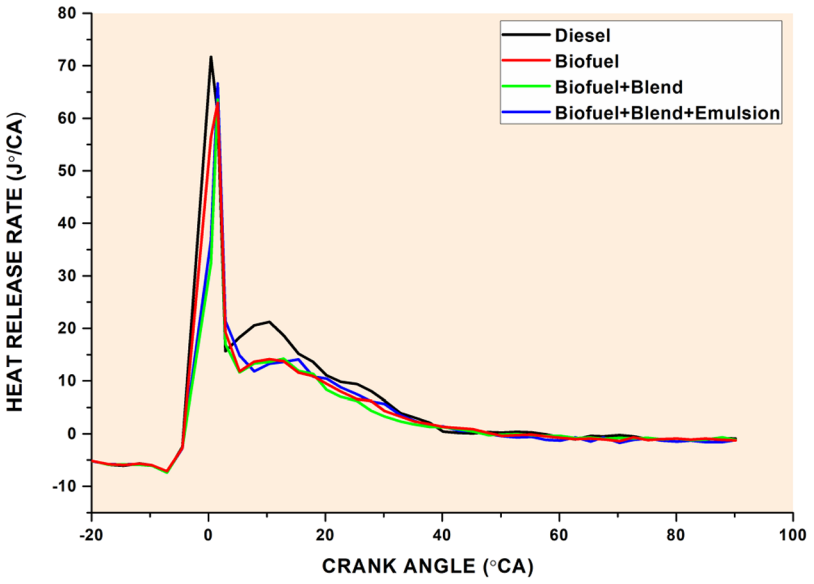

Figure 10. HRR for various fuel blends.

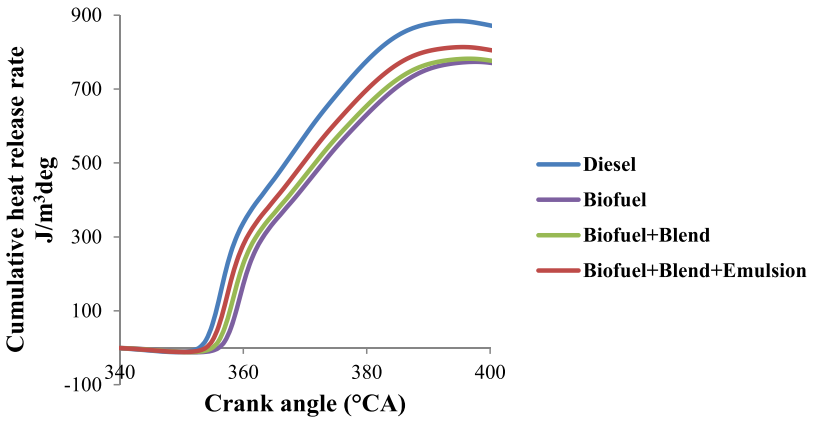

Figure 11. CHRR for various fuel blends.

$$\frac{dQ_n}{d\theta} = \left[\frac{\gamma}{\gamma - 1} P \frac{dV}{d\theta}\right] + \left[\frac{1}{\gamma - 1} V \frac{dP}{d\theta}\right] + Q_{lwg} \quad (2)$$

dQn = net heat release rate (J/°CA), θ = crank angle in degree, V = $d\theta$ instantaneous volume in m^3, = ratio in specific heats in C γ p/C_v (kJ/kg K), and P = instantaneous pressure in N/m^2, and Qlwg = blow by loss. The gross HRR was formulated as

$$\frac{dQ_L}{d\theta} = \frac{dQ_P}{d\theta} + \frac{dQ_{MW}}{d\theta} \quad (3)$$

The above equation denotes the gross heat transfer rate along the dQMW/$d\theta$ combustion chamber walls. The HRR at each crank angle was considered with the first law of thermodynamics and this equation model. Figure 10 displays the HRR variation for all the fuel blends to their crank angle. From the HRR plot, it was observed that the test fuel blends did not have a proper HRR curve throughout the entire crank angle, which was attained by the ignition delay period and more vaporization of the fuel blends. Figure 11 show that CHRR for various fuel blends.. Meanwhile, in the post-combustion process, the HRR peak had a positive range for all the fuel blends, which followed the same pattern as the diesel fuel blend. As evident from the literature, owing to better diffusion, a PCP, and the minimal cetane number of the fuel blends, a long ignition delay offers more fuel present in the combustion chamber. From the HRR plot, the test fuel blends (biofuel + blend + emulsion), biofuel + blend, and biofuel had a similar trend to diesel fuel blends at peak load, which might be caused by the higher cetane number, low fuel calorific value, and a quicker ignition delay period of the fuel blends. At 100% engine load, the HRR of diesel fuel is highest (71.71 J/m^3deg), followed by raw biofuel (62.97 J/m^3deg), emulsified biofuel (63.12 J/m^3deg), and nano additives appended to emulsified fuel (66.65 J/m^3deg). Conversely, the nanoparticle blended water/biofuel emulsion fuels reduce the HRR and corresponding CA due to reduced IDP. The presence of nanoparticles in the fuel reduces the fuel accumulation during the PCP and lowers the HRR.

4.5. Cumulative HRR. The highest cumulative heat release (CHRR) rates for the test fuels were 884.02, 813.45, 781.95, and 773.59 J for diesel, emulsified additive biofuel, emulsified biofuel, and biofuel, respectively. The improved qualities of diesel fuel result in greater atomization, which raises CHRR, which is why diesel has the greatest CHRR. Biofuel had the lowest CHRR, which was ascribed to its increased viscosity, which caused inappropriate atomization, poor air−fuel mixing,

https://doi.org/10.1021/acsomega.3c00325
ACS Omega 2023, 8, 18566−18581

and decreased combustion efficiency. The encapsulated nano additive water droplets in the biofuel emulsion fuel could have absorbed the heat rapidly, thereby decreasing the burning gas temperature inside the combustion chamber and improving the combustion rate homogenization of the reactant mixture, followed by the reduced EGT. Appending additives to emulsified biofuel tends to higher heat release significantly because the additives act as oxygen buffers during the combustion phase.[48−53]

4.6. Ignition Delay. In a CI engine, the ignition delay is often described as the interval between the start of injection and when 10% of the mass is burnt. As shown in Figure 12, at

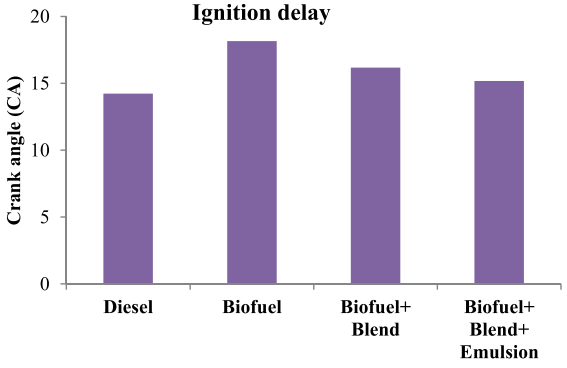

Figure 12. Ignition delay for various fuel blends.

100% load, the ignition delay periods were observed for diesel fuel (14.22 CA), emulsified biofuel (16.18 CA), biofuel (18.15 CA), and emulsified additive biofuel (15.18 CA). Due to higher water content, biofuel results in a prolonged ignition delay compared to neat diesel due to higher water content, which subsequently lowers the combustion chamber temperature. In addition, there is a reduction in combustion gas temperature by using water-emulsified fuel, thereby resulting in incomplete combustion.[54−62] Appending additives in emulsified biofuel results in shortened ignition delay compared to other biofuels because the additive acts as an oxygen buffer during the combustion process, thereby lowering the possibility of unburned fraction formation. The intensive secondary atomization and significant fuel distribution in nano additives and emulsion in the combustion chamber result in reduced ignition delay. In response to these effects, there was a marginal reduction in exhaust emissions and there was significantly improved fuel homogenization in the combustion chamber in response to the addition of the nano additives. The researchers claimed that the better mixing of air and fuel was due to the inclusion of carbon-based nanoparticles. They claimed that by inducing micro explosions and oxygenic functional groups on the particles, the nano additives had a positive impact on the combustion process.

4.7. Combustion Phasing. The combustion phasing angle (CA 50) refers to the crank angle at which 50% of the heat has reportedly been emitted.

At 100% load, the combustion phasing angles were observed for diesel fuel (368 CA), emulsified biofuel (372 CA), biofuel (373 CA), and emulsified additive biofuel (370 CA). The combustion center is one of the most important parameters affecting engine efficiency and emissions. It can be defined as the crank angle of 50% combustion mass fraction (CA50). Figure 13 shows the change of CA50 for various test fuels. With the delay of ignition timing, CA50 is delayed from TDC.

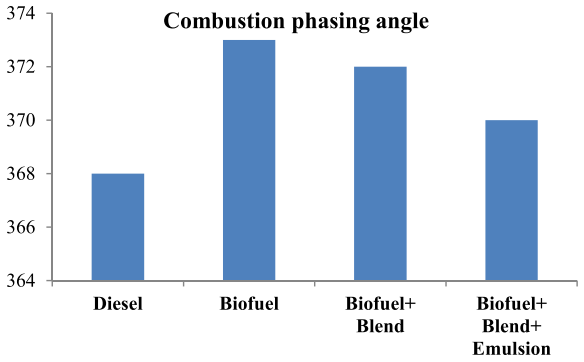

Figure 13. Combustion phasing angle for various fuel blends.

It is shown in the figure that the nano additive emulsion enhances the combustion speed near the diesel and advances the combustion center. The intensive secondary atomization and significant fuel distribution in nano additives and emulsion in the combustion chamber result in reduced ignition delay.

4.8. Combustion Duration. The time between 10 and 90% of the mass fraction burned is considered the combustion duration of a CI engine. From Figure 14, at 100% load, the

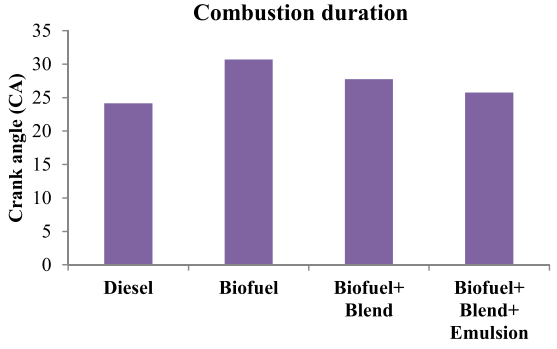

Figure 14. Combustion duration for various fuel blends.

combustion phasing angles were observed for diesel fuel (24.15 CA), emulsified biofuel (27.76 CA), biofuel (30.68 CA), and emulsified additive biofuel (25.7 CA). The prolonged combustion duration among the test fuel is biofuel, which attributes to higher water content subsequently lowering the combustion chamber temperature. Appending additives in emulsified biofuel results in shortened combustion duration compared to other biofuels because the additive acts as an oxygen buffer during the combustion process, thereby shortening the ignition delay, and subsequently enhances combustion temperature thereby lowering the possibility of unburned fraction formation. The intensive secondary atomization and significant fuel distribution in nano additives and emulsion in the combustion chamber result in reduced combustion duration. In response to these effects, there was a marginal advancement in the combustion phasing angle. Meanwhile, water increases combustion duration due to the oxidation of soot by the OH radicals in the latter phase of combustion. The presence of nanoparticles in the emulsion fuels reduces the delay period, resulting in a lower HRR than plain emulsion fuels.

4.9. HC. HC and CO emissions from diesel engines are critical parameters for analyzing their performance and emission characteristics. As shown in Figure 15, at 100% load, the highest HC emissions were observed for diesel fuel

https://doi.org/10.1021/acsomega.3c00325
ACS Omega 2023, 8, 18566−18581

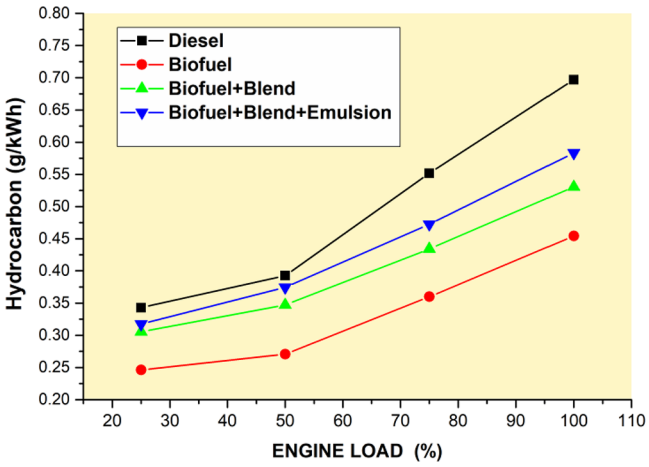

Figure 15. HC emission for various fuel blends.

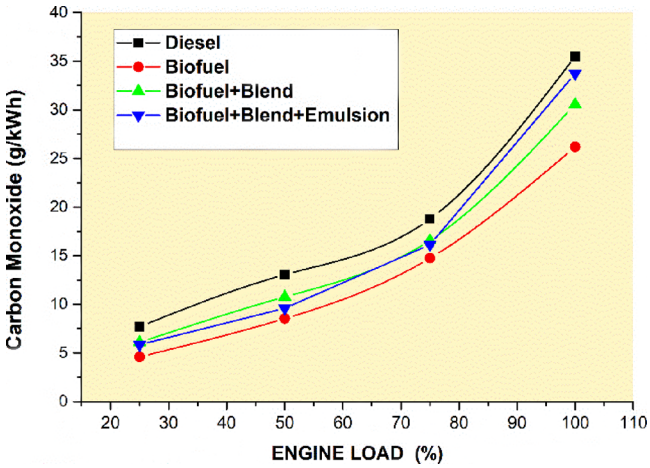

Figure 16. CO emission for various fuel blends.

(0.69 g/kWh), emulsified biofuel (0.58 g/kWh), biofuel (0.53 g /kWh), and emulsified additive biofuel (0.45 g/kWh). With an increase in engine load, HC emissions increase due to more fuel being supplied to the engine cylinder. Factors responsible for HC emission formation are improper fuel−air mixing, wall impingement, quenching, poor air entrainment, quenching on cylinder walls, etc. Due to more oxygen present in biofuel, clean biofuel results in the lowest HC emissions throughout the engine load compared to diesel fuel. Due to higher water content, emulsified biofuel results in a higher HC emulsion compared to neat biofuel due to higher water content, which subsequently lowers the combustion chamber temperature. In addition, there is a reduction in combustion gas temperature by using water-emulsified fuel, thereby resulting in incomplete combustion. Appending additives in emulsified biofuel results in lowered HC emissions compared to other test fuels because the additive acts as an oxygen buffer during the combustion process, thereby lowering the possibility of unburned fraction formation. Due to the intensive secondary atomization and significant fuel distribution in nano additives and emulsion in the combustion chamber, resulting in HC oxidation, the addition of nano additives with emulsion blend reduced HC emissions by 20.68%. In response to these effects, there was a marginal reduction in HC emissions and micro-explosion phenomena and there was significantly improved fuel homogenization in the combustion chamber in response to the addition of the nano additives. The researchers claimed that the better mixing of air and fuel was due to the inclusion of carbon-based nanoparticles. They claimed that by inducing micro explosions and oxygenic functional groups on the particles, the nano additives had a positive impact on the combustion process and HC emissions. The differences observed between these reports and those of the present study could be attributed to the differences in fuel types, fuel nano additives used, and particle sizes.

4.10. CO. CO formation is very typical in diesel engines. The main reason for the CO formation is the dissociation process, where the carbon dioxide dissociates into CO and a single oxygen molecule. As shown in Figure 16, it is observed that emulsified biofuel exhibits the lowest CO emissions owing to a higher rate of combustion. Raw biofuel has the lowest CO emission compared to diesel fuel due to the presence of oxygen content in raw fuel. However, the emulsified biofuel results in higher CO emissions than raw biofuel, which accounts for the higher latent heat of vaporization of a water molecule in an emulsified blend, thereby lowering the cylinder temperature and leading to higher CO emissions. Appending additives in an emulsified blend leads to lower CO emissions in comparison with other test fuels. This could be attributed to the oxidation capability of additives that act as oxygen buffers, thereby causing more CO molecules to react with oxygen, subsequently forming carbon dioxide molecules and lowering the possibility of CO formation. The biofuel + blend + emulsion fuel had a 7.83% decline in CO_2 emissions compared with diesel fuel at peak load. This could happen if the catalytic benefits of the nano additives compensated for their unfavorable impacts concerning the increased carbon content of the fuel blend. Globally, the researchers also highlighted the positive impacts of carbon nano additives in water/biodiesel emulsions on increasing fuel−air mixing and consequently lowering the ignition delay, resulting in reduced CO emissions. Besides, this could be the attribute of higher IDP and enhanced surface-area-to-volume ratio associated with nanoparticles blended into emulsion fuel.[63−66]

4.11. Oxides of Nitrogen (NO_x). It is observed that raw biofuel exhibits the highest NO_x emissions in comparison with other test fuels, owing to excess oxygenates in the fuel, which enhances the combustion rate significantly. Moreover, higher levels of engine output result in higher peak in-cylinder temperatures inside the cylinder, thereby resulting in higher NO_x formation. It is also observed that biofuel combustion exhibits higher NO_x emissions than diesel fuel while emulsified biofuel results in lower NO_x emissions than neat biofuel, which could be attributed to the presence of water molecules lowering the temperature inside the combustion chamber. The latent heat of the water will cool the charge due to the evaporation of water, and the cylinder temperature will be subsequently lowered, thus resulting in lower peak combustion temperatures. In Figure 17, adding additives to emulsified biofuel lowered NO_x emissions more than all the test fuels. Compared with diesel fuel, NO_x emissions are reduced by 20.82% for emulsified additive fuel and NO_x emissions are increased for raw biofuel and emulsified fuel by about 5.84 and 2.46%, respectively, at 100% engine load condition. The nearly 27.7% reduction of NO_x emissions for nano additives blended into biofuel + blend fuel blends could be ascribed to the chemical activity of nano additives catalyzing, and the decrements in NO_x formation as a consequence of the

https://doi.org/10.1021/acsomega.3c00325
ACS Omega 2023, 8, 18566−18581

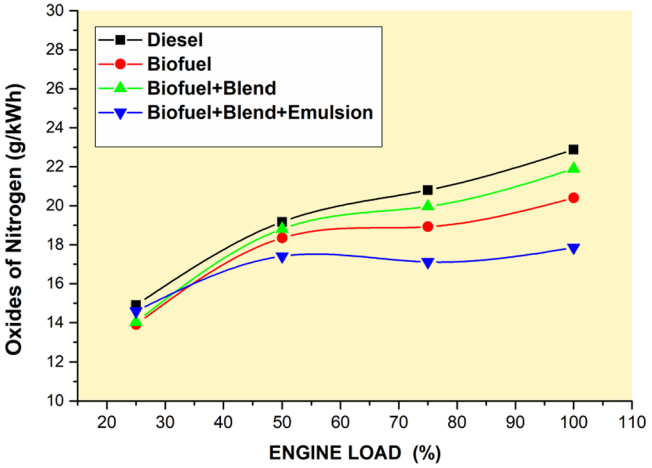

Figure 17. NO_x emission for various fuel blends.

presence of nano additives in water/biofuel emulsion fuels have been previously reported as well. The higher latent heat of water vaporization results in a heat sink, which lowers the in-cylinder temperature and therefore causes a reduction in NO_x emission.

4.12. Smoke Emissions. The main contributor to the smoke emissions is the fuel-rich zones present inside the engine cylinder. The highest smoke emissions were observed for diesel fuel throughout the engine load condition. As shown in Figure 18, it can be observed that the biofuel-blended fuel

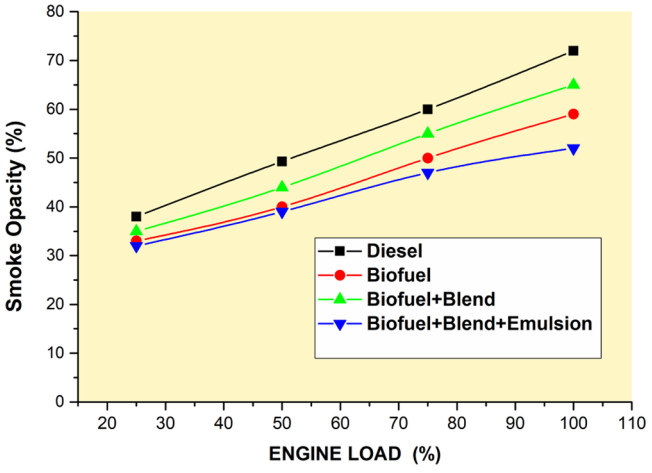

Figure 18. Smoke emission for various fuel blends.

exhibits lower smoke emissions in comparison with diesel fuel by 21.3, 12, and 37.3%, respectively, at higher loads owing to the presence of oxygen content in the test fuel. Moreover, the emulsified biofuel exhibits much lower smoke than neat biofuel due to the micro-explosion phenomenon, and differences in volatility among the water and fuel molecules improve the air–fuel mixing and lower the soot formation subsequently. This typical smoke reduction may also be attributed to the "dilution effect" caused by steam generation because of water in the emulsified fuel and physical and chemical effects such as mixing improvements and water–gas reaction. Appending additives to emulsified biofuel tends to lower the smoke significantly because the additives act as oxygen buffers during the combustion phase. This can be attributed to partial oxidation of fuel mixtures, which lowers the over-rich zones, limiting the primary smoke formation. Because they promote shorter IDP and improved combustion characteristics, nanoparticles blended into water/biofuel emulsion fuels further reduce the magnitude of smoke opacity. The nanoparticles' inclusion does not react with the fuel during the combustion process. The nanoparticle enhances the heat transfer properties during the combustion process and escapes to the atmosphere through the engine exhaust. The proper mixing of air and fuel and the significantly shortened ignition delay attribute the better result of the reduced intensity of smoke opacity to the volatility and high cetane number. In addition, the occurrence of reduced soot formation and improved reactant mixture is due to the immediate secondary atomization effects of nano additives in the fuel blends.

5. CONCLUSIONS

The current experimental work analyses the diesel engine's performance, combustion, and emission characteristics fueled with diesel, biofuel, emulsified biofuel, and additives blended with emulsified biofuel. Experiments were conducted at five engine load intervals of 0, 25, 50, 75, and 100%, respectively. Based on the experimentation, the following conclusions were drawn subsequently:

- Appending additives in the emulsified fuel has improved the BTE and BSEC. At full load, the BTE and BSEC of appended emulsified BMWCNT fuel achieved 13.6% higher fuel consumption and 4.7% lower thermal efficiency than mineral diesel.
- Emissions-wise, for appended emulsified fuel, there is a significant drop in HC and CO emissions by about 20.68 and 7.83%, while the NO_x emissions were reduced by about 27.7% in comparison with diesel fuel. Similarly, a typical smoke reduction of about 37.3% was observed for additives appended to emulsified fuel.

AUTHOR INFORMATION

Corresponding Author

Arularasu Sivalingam – *Department of Automobile Engineering, SAMS College of Engineering and Technology, Chennai, Tamil Nadu 600013, India*; orcid.org/0000-0002-9176-1803; Email: arularasus3@gmail.com

Authors

Elumalai Perumal Venkatesan – *Department of Mechanical Engineering, Aditya Engineering College, Surampalem 533437, India*

Kenneth L. Roberts – *College of Engineering and Computing, University of South Carolina, Columbia, South Carolina 29208, United States*

Mohammad Asif – *Department of Chemical Engineering, College of Engineering, King Saud University, Riyadh 12372, Saudi Arabia*

Complete contact information is available at: https://pubs.acs.org/10.1021/acsomega.3c00325

Notes

The authors declare no competing financial interest.

ACKNOWLEDGMENTS

The financial support from the Researchers Supporting Project (RSP2023R42), King Saud University, Riyadh, Saudi Arabia is appreciated.

https://doi.org/10.1021/acsomega.3c00325
ACS Omega 2023, 8, 18566–18581

REFERENCES

(1) Mahmudul, H. M.; Hagos, F. Y.; Mamat, R.; Adam, A. A.; Ishak, W. F. W.; Alenezi, R. Production , characterization and performance of biodiesel as an alternative fuel in diesel engines − A review. *Renewable Sustainable Energy Rev.* **2017**, *72*, 497−509.

(2) Chandrasekaran, V.; Arthanarisamy, M.; Nachiappan, P.; et al. The role of nano additives for biodiesel and diesel blended transportation fuels. *Transp. Res. D: Transp. Environ.* **2016**, *46*, 145−156.

(3) Ramalingam, K; Research Scholar, M, Kandasamy Associate professor A et al. (2018). *An assessment of combustion, performance characteristics and emission control strategy by adding anti-oxidant additive in emulsified fuel*; Atmospheric Pollution Research 1−0. DOI: 10.1016/j.apr.2018.02.007

(4) Javed, S.; Satyanarayana Murthy, Y. V. V.; Satyanarayana, M. R. S.; Rajeswara Reddy, R.; Rajagopal, K. Effect of a zinc oxide nanoparticle fuel additive on the emission reduction of a hydrogen dual-fuelled engine with jatropha methyl ester biodiesel blends. *J. Cleaner Prod.* **2016**, *137*, 490−506.

(5) Dong, T.; Fei, Q.; Genelot, M.; et al. A novel integrated biorefinery process for diesel fuel blendstock production using lipids from the methanotroph, Methylomicrobium buryatense. *Energy Convers. Manage.* **2017**, *140*, 62−70.

(6) Amini, Z.; Ilham, Z.; Chyuan, H.; et al. State of the art and prospective of lipasecatalyzed transesterification reaction for biodiesel production. *Energy Convers. Manage.* **2017**, *141*, 339−353.

(7) Takase, M.; Zhao, T.; Zhang, M.; et al. An expatiate review of neem, jatropha, rubber and karanja as multipurpose non-edible biodiesel resources and comparison of their fuel, engine and emission properties. *Renewable Sustainable Energy Rev.* **2015**, *43*, 495−520.

(8) Fukuda, H.; Kondo, A.; Noda, H. Biodiesel fuel production by transesterification of oils. *J. Biosci. Bioeng.* **2001**, *92*, 405−416.

(9) Vijayaraj, K.; Sathiyagnanam, A. P. Experimental investigation of a diesel engine with methyl ester of mango seed oil and diesel blends. *Alexandria Eng. J.* **2016**, *55*, 215−221.

(10) Sridharan, G.; Chandramouli, R.; Musthafa, M. M.; Ashok Kumar, T. Performance, combustion and emission characteristics of a single cylinder CI engine running on diesel-biodiesel-water emulsion with additive. *Energy Sources, Part A* **2019**, *7036*, 1.

(11) Prabhu, A.; Venkata Ramanan, M. A comprehensive review of water injection and emulsion technology for biodiesel-fuelled CI engine. *Int. J. Ambient Energy* **2021**, *42*, 720−724.

(12) Vellaiyan, S.; Amirthagadeswaran, K. S. The role of water-in-diesel emulsion and its additives on diesel engine performance and emission levels : A retrospective review. *Alexandria Eng. J.* **2016**, *55*, 2463−2472.

(13) Vellaiyan, S.; Subbiah, A.; Chockalingam, P. Effect of Titanium dioxide nanoparticle as an additive on the working characteristics of biodiesel-water emulsion fuel blends. *Energy Sources, Part A* **2021**, *43*, 1087−1099.

(14) Lin, J.; Gaustad, G.; Trabold, T. A. Profit and policy implications of producing biodiesel-ethanol-diesel fuel blends to specification. *Appl. Energy* **2013**, *104*, 936−944.

(15) Ashok, B.; Thundil Karuppa Raj, R.; Nanthagopal, K.; et al. Lemon peel oil − A novel renewable alternative energy source for diesel engine. *Energy Convers. Manage.* **2017**, *139*, 110−121.

(16) Purushothaman, K.; Nagarajan, G. Performance, emission and combustion characteristics of a compression ignition engine operating on neat orange oil. *Renewable Energy* **2009**, *34*, 242−245.

(17) Vallinayagam, R.; Vedharaj, S.; Yang, W. M.; et al. Impact of ignition promoting additives on the characteristics of a diesel engine powered by pine oil-diesel blend. *Fuel* **2014**, *117*, 278−285.

(18) Dhinesh, B.; Isaac JoshuaRamesh Lalvani, J.; Parthasarathy, M.; Annamalai, K. An assessment on performance, emission and combustion characteristics of single cylinder diesel engine powered by Cymbopogon flexuosus biofuel. *Energy Convers. Manage.* **2016**, *117*, 466−474.

(19) Vallinayagam, R.; Vedharaj, S.; Yang, W. M.; et al. Feasibility of using less viscous and lower cetane (LVLC) fuels in a diesel engine: A review. *Renewable Sustainable Energy Rev.* **2015**, *51*, 1166−1190.

(20) Devan, P. K.; Mahalakshmi, N. V. A study of the performance, emission and combustion characteristics of a compression ignition engine using methyl ester of paradise oil-eucalyptus oil blends. *Appl. Energy* **2009**, *86*, 675−680.

(21) Silitonga, A. S.; Masjuki, H. H.; Ong, H. C.; et al. Synthesis and optimization of Hevea brasiliensis and Ricinus communis as feedstock for biodiesel production: A comparative study. *Ind. Crops Prod.* **2016**, *85*, 274−286.

(22) Yang, W. M.; An, H.; Chou, S. K.; et al. Impact of emulsion fuel with nano-organic additives on the performance of diesel engine. *Appl. Energy* **2013**, *112*, 1206−1212.

(23) Prabhu, L; Kumar, SS; Rajan, AAK (2015) National Conference On Recent Trends And Developments In *Sustainable Green Technologies Investigation On Performance And Emission Analysis Of Tio2 Nanoparticle As An Additive For Bio-Diesel Blends National Conference On Recent Trends And Developments* In . 408−412

(24) Verma, P.; Sharma, M. P.; Dwivedi, G. Impact of alcohol on biodiesel production and properties. *Renewable Sustainable Energy Rev.* **2016**, *56*, 319−333.

(25) Selvakumar, P.; Sivashanmugam, P. Optimization of lipase production from organic solid waste by anaerobic digestion and its application in biodiesel production. *Fuel Process. Technol.* **2017**, *165*, 1−8.

(26) Ciftci, O. N.; Temelli, F.; Fjerbaek, L.; et al. Optimization of lipase production from organic solid waste by anaerobic digestion and its application in biodiesel production. *Energy Convers. Manage.* **2016**, *102*, 2130−2134.

(27) Nair, J. N.; Kaviti, A. K.; Daram, A. K. Analysis of performance and emission on compression ignition engine fuelled with blends of Neem biodiesel. *Egypt. J. Pet.* **2017**, *26*, 927−931.

(28) Subramanian, T.; Geo, V. E.; Martin, L. J. Mitigation of carbon footprints through a blend of biofuels and oxygenates , combined with post-combustion capture system in a single cylinder CI engine. *Renewable Energy* **2019**, *130*, 1067−1081.

(29) Patel, P. D.; Lakdawala, A.; Chourasia, S.; Patel, R. N. Bio fuels for compression ignition engine: A review on engine performance, emission and life cycle analysis. *Renewable Sustainable Energy Rev.* **2016**, *65*, 24−43.

(30) Dhinesh, B.; Niruban Bharathi, R.; Isaac JoshuaRamesh Lalvani, J.; et al. An experimental analysis on the influence of fuel borne additives on the single cylinder diesel engine powered by Cymbopogon flexuosus biofuel. *J. Energy Inst.* **2017**, *90*, 634−645.

(31) Jaichandar, S.; Annamalai, K. Combined impact of injection pressure and combustion chamber geometry on the performance of a biodiesel fueled diesel engine. *Energy.* **2013**, 330.

(32) Mehta, R. N.; Chakraborty, M.; Parikh, P. A. Impact of hydrogen generated by splitting water with nano-silicon and nano-aluminum on diesel engine performance. *Int. J. Hydrogen Energy* **2014**, *39*, 8098−8105.

(33) Shaafi, T.; Sairam, K.; Gopinath, A.; et al. Effect of dispersion of various nanoadditives on the performance and emission characteristics of a CI engine fuelled with diesel, biodiesel and blends—A review. *Renewable Sustainable Energy Rev.* **2015**, *49*, 563−573.

(34) Mirzajanzadeh, M.; Tabatabaei, M.; Ardjmand, M.; Rashidi, A.; Ghobadian, B.; Barkhi, M.; Pazouki, M. A novel soluble nanocatalysts in diesel − biodiesel fuel blends to improve diesel engines performance and reduce exhaust emissions. *Fuel* **2015**, *139*, 374−382.

(35) Purohit, R.; Purohit, K.; Rana, S.; Rana, R. S.; Patel, V. Carbon Nanotubes and Their Growth Methods. *Procedia Mater. Sci.* **2014**, *6*, 716−728.

(36) Ahn, K.; Kim, S.; Yu, J. Multi-Walled Carbon Nanotube (MWCNT) Dispersion and Aerosolization with Hot Water Atomization without Addition of Any Surfactant. *Safety and Health at Work* **2011**, *2*, 65−69.

(37) Hazar, H.; Sevinc, H. nvestigation of exhaust emissions and performance of a diesel engine fueled with preheated raw grape seed

https://doi.org/10.1021/acsomega.3c00325
ACS Omega 2023, 8, 18566−18581

oil/propanol blends. *Chemical Engineering and Processing - Process Intensification* **2023**, *188*, 109378.
(38) Venu, H.; Madhavan, V. Effect of Al_2O_3nanoparticles in biodiesel-diesel-ethanol blends at various injection strategies: Performance, combustion and emission characteristics. *Fuel* **2016**, *186*, 176−189.
(39) El-batal, A. I.; Farrag, A. A.; Elsayed, M. A.; El-khawaga, A. M. Biodiesel Production by Aspergillus niger Lipase Immobilized on Barium Ferrite Magnetic Nanoparticles. 2016, DOI: 10.3390/bioengineering3020014.
(40) Balasubramanian, D.; Sokkalingam Arumugam, S. R.; Subramani, L.; Joshua Stephen Chellakumar, I. J. R. L.; Mani, A. A numerical study on the effect of various combustion bowl parameters on the performance, combustion, and emission behavior on a single cylinder diesel engine. *Environ. Sci. Pollut. Res.* **2018**, *25*, 2273−2284.
(41) Yang, W. M.; An, H.; Chou, S. K.; et al. Emulsion fuel with novel nano-organic additives for diesel engine application. *Fuel* **2013**, *104*, 726−731.
(42) Sadhik Basha, J.; Anand, R. B. The influence of nano additive blended biodiesel fuels on the working characteristics of a diesel engine. *J. Braz. Soc. Mech. Sci. Eng.* **2013**, *35*, 257−264.
(43) Afzal, A.; Aabid, A.; Khan, A.; Khan, S. A.; Rajak, U.; Verma, T. N.; Kumar, R. Response surface analysis, clustering, and random forest regression of pressure in suddenly expanded high-speed aerodynamic flows. *Aerosp. Sci. Technol.* **2020**, *107*, No. 106318.
(44) Afzal, A.; Ansari, Z.; Faizabdi, A. R.; Ramis, M. K. Parallelization Strategies for Computational Fluid Dynamics Software: State of the Art Review. *Arch. Comput. Methods Eng.* **2017**, *24*, 337−363.
(45) Afzal, A.; Mujeebu, M. A. Thermo-Mechanical and Structural Performances of Automobile Disc Brakes: A Review of Numerical and Experimental Studies. *Arch. Comput. Methods Eng.* **2019**, *26*, 1489−1513.
(46) Pinto, R. N.; Afzal, A.; D'Souza, L. V.; Ansari, Z.; Samee, A. D. M. Computational Fluid Dynamics in Turbomachinery: A Review of State of the Art. *Arch. Comput. Methods Eng.* **2017**, *24*, 467−479.
(47) Jilte, R.; Afzal, A.; Panchal, S. A novel battery thermal management system using nano-enhanced phase change materials. *Energy* **2021**, *219*, No. 119564.
(48) Ağbulut, Ü.; Sarıdemir, S.; Rajak, U.; Polat, F.; Afzal, A.; Verma, T. N. Effects of high-dosage copper oxide nanoparticles addition in diesel fuel on engine characteristics. *Energy* **2021**, *229*, No. 120611.
(49) Afzal, A.; Bhutto, J. K.; Alrobaian, A.; Kaladgi, A. R.; Khan, S. A. Modelling and Computational Experiment to Obtain Optimized Neural Network for Battery Thermal Management Data. *Energies* **2021**, *14*, 7370.
(50) Mokashi, I.; Afzal, A.; Khan, S. A.; Abdullah, N. A.; Bin Azami, M. H.; Jilte, R.; Samuel, O. D. Nusselt number analysis from a battery pack cooled by different fluids and multiple back-propagation modelling using feed-forward networks. *Int. J. Therm. Sci.* **2021**, *161*, No. 106738.
(51) Chandrashekar, A.; Chaluvaraju, B.; Afzal, A.; Vinnik, D.; Kaladgi, A.; Alamri, S. C. A. A.; Tirth, V. Mechanical and Corrosion Studies of Friction Stir Welded Nano Al_2O_3 Reinforced Al-Mg Matrix Composites: RSM-ANN Modelling Approach. *Symmetry* **2021**, *13*, 537.
(52) Afzal, A.; Khan, S. A.; Saleel, C. A. Role of ultrasonication duration and surfactant on characteristics of ZnO and CuO nanofluids. *Mater. Res. Express* **2019**, *6*, 1150d8.
(53) Afzal, A.; Nawfal, I.; Mahbubul, I. M.; Kumbar, S. S. An overview on the effect of ultrasonication duration on different properties of nanofluids. *J. Therm. Anal. Calorim.* **2019**, *135*, 393−418.
(54) Afzal, A.; Yashawantha, K. M.; Aslfattahi, N.; Saidur, R.; Razak, R. K. A.; Subbiah, R. Back propagation modeling of shear stress and viscosity of aqueous Ionic-MXene nanofluids. *J. Therm. Anal. Calorim.* **2021**, *145*, 2129−2149.
(55) Bakır, H.; Ağbulut, Ü.; Gürel, A. E.; Yıldız, G.; Güvenç, U.; Soudagar, M. E. M.; Hoang, A. T.; Deepanraj, B.; Saini, G.; Afzal, A. Forecasting of future greenhouse gas emission trajectory for India using energy and economic indexes with various metaheuristic algorithms. *J. Cleaner Prod.* **2022**, *360*, No. 131946.
(56) Samuel, O. D.; Waheed, M. A.; Taheri-Garavand, A.; Verma, T. N.; Dairo, O. U.; Bolaji, B. O.; Afsal, A. Prandtl number of optimum biodiesel from food industrial waste oil and diesel fuel blend for diesel engine. *Fuel* **2021**, *285*, No. 119049.
(57) Samuel, O. D.; Okwu, M. O.; Oyejide, O. J.; Taghinezhad, E.; Afzal, A.; Kaveh, M. Optimizing biodiesel production from abundant waste oils through empirical method and grey wolf optimizer. *Fuel* **2020**, *281*, No. 118701.
(58) Sharath, B. N.; Venkatesh, C. V.; Afzal, A.; Aslfattahi, N.; Aabid, A.; Baig, M.; Saleh, B. Multi Ceramic Particles Inclusion in the Aluminium Matrix and Wear Characterization through Experimental and Response Surface-Artificial Neural Networks. *Materials* **2021**, *14*, 2895.
(59) Afzal, A.; Saleel, C. A.; Badruddin, I. A.; Khan, T. Y.; Kamangar, S.; Mallick, Z.; Samuel, O. D.; Soudagar, M. E. Human thermal comfort in passenger vehicles using an organic phase change material—An experimental investigation, neural network modelling, and optimization. *Build. Environ.* **2020**, *180*, No. 107012.
(60) Afzal, A.; Mokashi, I.; Khan, S. A.; Abdullah, N. A.; Bin Azami, M. H. Optimization and analysis of maximum temperature in a battery pack affected by low to high Prandtl number coolants using response surface methodology and particle swarm optimization algorithm. *Numer. Heat Transfer, Part A* **2021**, *79*, 406−435.
(61) Afzal, A.; Khan, S. A.; Islam, T.; Jilte, R. D.; Khan, A.; Soudagar, M. E. M. Investigation and back-propagation modeling of base pressure at sonic and supersonic Mach numbers. *Phys. Fluids* **2020**, *32*, No. 096109.
(62) Sathish, T.; Kaladgi, A. R. R.; Mohanavel, V.; Arul, K.; Afzal, A.; Aabid, A.; Baig, M.; Saleh, B. Experimental Investigation of the Friction Stir Weldability of AA8006 with Zirconia Particle Reinforcement and Optimized Process Parameters. *Materials* **2021**, *14*, 2782.
(63) Afzal, A.; Mohammed Samee, A. D.; Javad, A.; Shafvan, S. A.; Ajinas, P. V.; Ahammedul Kabeer, K. M. Heat transfer analysis of plain and dimpled tubes with different spacings. *Heat Transfer* **2018**, *47*, 556−568.
(64) Elumalai, P. V.; Parthasarathy, M.; Murugan, M.; Saravanan, A.; Sivakandhan, C. Effect of Cerium Oxide Nanoparticles to Improve the Combustion Characteristics of Palm Oil Nano Water Emulsion Using Low Heat Rejection Engine. *Int. J. Green Energy* **2021**, *18*, 1482−1496.
(65) Elumalai, P. V.; Balasubramanian, D.; Parthasarathy, M.; Pradeepkumar, A. R.; Mohamed Iqbal, S.; Jayakar, J.; Nambiraj, M. An Experimental Study on Harmful Pollution Reduction Technique in Low Heat Rejection Engine Fuelled with Blends of Pre-Heated Linseed Oil and Nano Additive. *J. Cleaner Prod.* **2021**, *283*, No. 124617.
(66) Elumalai, P. V.; Annamalai, K.; Dhinesh, B. Effects of Thermal Barrier Coating on the Performance, Combustion and Emission of DI Diesel Engine Powered by Biofuel Oil−Water Emulsion. *J. Therm. Anal. Calorim.* **2019**, *137*, 593−605.

https://doi.org/10.1021/acsomega.3c00325
ACS Omega 2023, 8, 18566−18581